GEOPHYSICAL RESEARCH LETTERS, VOL. 40, 676–680, doi:10.1029/2012GL053873, 2013

Inferring the depth of the zonal jets on Jupiter and Saturn from odd gravity harmonics

Yohai Kaspi[1]

Received 15 September 2012; revised 10 December 2012; accepted 13 December 2012; published 22 February 2013.

[1] The low-order even gravity harmonics J_2, J_4, and J_6 are well constrained for Jupiter and Saturn from spacecraft encounters over the past few decades. These gravity harmonics are dominated by the oblate shape and radial density distribution of these gaseous planets. In the lack of any north–south asymmetry, odd gravity harmonics will be zero. However, the winds on these planets are not hemispherically symmetric, and therefore can contribute to the odd gravity harmonics through dynamical variations to the density field. Here it is shown that even relatively shallow winds (reaching ~40 bars) can cause considerable odd gravity harmonics that can be detectable by NASA's Juno and Cassini missions to Jupiter and Saturn. Moreover, these measurements will have better sensitivity to the odd harmonics than to the high-order even harmonics, which have been previously proposed as a proxy for deep winds. Determining the odd gravity harmonics will therefore help constrain the depth of the jets on these planets, and may provide valuable information about the planet's core and structure. **Citation:** Kaspi, Y. (2013), Inferring the depth of the zonal jets on Jupiter and Saturn from odd gravity harmonics, *Geophys. Res. Lett., 40*, 676–680, doi: 10.1029/2012GL053873.

1. Introduction

[2] Jupiter and Saturn are large gas planets with no solid surface down to perhaps a small core [*Guillot*, 2005]. Because of their rapid rotation, their shape is distorted from perfect sphericity resulting in large gravity harmonics. To date, only the first three even zonal gravity harmonics J_2, J_4, and J_6 have been accurately measured [*Jacobson*, 2003; *Jacobson et al*., 2006], putting strong constraints on the interior mass distribution of these planets [e.g., *Guillot and Morel*, 1995]. In 2016, NASA's Juno mission will arrive at Jupiter equipped to perform high precision measurements of the gravity field with sensitivity at least up to J_{12} [*Bolton*, 2005]. These measurements should be able to provide strong constraints on the depth to which atmospheric circulation penetrates on these planets [*Hubbard*, 1999; *Kaspi et al*., 2010]. Coincidentally at the same time, NASA's Cassini mission will conclude its decade-long survey of the Saturnian system (the last part of the mission is coined the Cassini Solstice mission), with proximal orbits of Saturn obtaining the same type of data for Saturn, before the spacecraft terminates its operation by descending into Saturn's interior.

[3] At the visible cloud level, the atmospheric dynamics on these planets are dominated by strong east-west (zonal) jet streams [*Vasavada and Showman*, 2005]. It is currently unknown how deep these jets extend, and the only available data are from the Galileo entry probe to Jupiter that found $160\,\mathrm{m\,s^{-1}}$ winds extending down at least to 22 bars at the entry point of the probe [*Atkinson et al*., 1996]. For the Jupiter case, if strong winds extend to depths of more than 1000 km (~5000 bars), then they should have a significant effect on the high gravity harmonics [*Hubbard*, 1999; *Kaspi et al*., 2010]. This is caused because the dynamical density variations that are in balance with the winds, perturb the mass distribution on the planets, and affect the gravity spectrum. For the lower harmonics, this perturbation has a much smaller effect on the harmonics than that caused by the oblateness and compressibility of the planet. However, as first noted by Hubbard [1999], beyond degree 10, the dynamical perturbations will dominate the gravity spectrum.

[4] Because Jupiter and Saturn are gaseous, aside from the cloud-level winds, there is no apparent asymmetry between the northern and southern hemisphere. Therefore, the gravitational harmonics resulting from the shape and vertical structure of the planets have identically zero odd harmonics. However, the observed cloud level wind structure does have hemispherical differences (Figure 1), and therefore, the contribution to the odd gravity harmonics due to wind should be nonzero. Unlike the even harmonics that have a contribution from both the solid-body density distribution and the dynamics, the odd harmonics are caused therefore *purely* due to dynamics. Thus, any odd signal detected will be a sign of a dynamical contribution to the gravity signal. This paper attempts to estimate how large these odd harmonics can be, and investigate whether they can be measured by Juno and Cassini.

2. The Gravity Signal of Internal Dynamics

[5] The interior density distribution of the planet determines the zonal gravity harmonics which can be defined as

$$J_n = -\frac{1}{Ma^n}\int P_n \rho r^n d^3\mathbf{r}, \tag{1}$$

where M is the planetary mass, a is the mean radius, P_n is the n-th Legendre polynomial, and ρ is the local density [*Hubbard*, 1984]. The density can be divided into a solid-body component $\widetilde{\rho}(r,\theta)$ and a dynamical component $\rho'(r,\theta)$ arising from the fluid motion relative to the static rotating planet (r is radius and θ is latitude), so that $\rho = \widetilde{\rho} + \rho'$. Thus, in the lack of any flow, ρ' vanishes, and J_n reduces to the harmonics arising from only the shape and radial density

[1]Department of Environmental Sciences and the Center for Planetary Science, Weizmann Institute of Science, Rehovot, Israel.

Corresponding author: Yohai Kaspi, Department of Environmental Sciences and the Center for Planetary Science, Weizmann Institute of Science, Rehovot, 76100, Israel. (yohai.kaspi@weizmann.ac.il)

0094-8276/13/2012GL053873

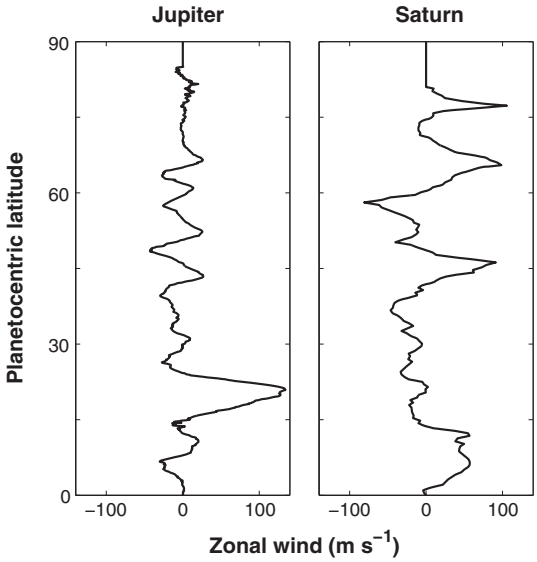

Figure 1. The difference between the northern and southern hemisphere cloud-level zonal wind (m s^{-1}) as function of latitude for Jupiter (left) and Saturn (right). The total cloud-level zonal wind is shown in Figure 2a.

distribution of the planet [*Zharkov and Trubitsyn*, 1978; *Hubbard*, 2012]. If the planet would have been completely spherical the radial profile of density alone will have no projection on P_n for $n > 1$ in equation 1, and all the harmonics will vanish. However, the oblateness of Jupiter and Saturn, given as the difference between polar and equatorial radius, is 6.5% and 9.8%, respectively [*Seidelmann et al.*, 2007], and therefore, they have considerable zonal harmonics. Since the mean density distribution is hemispherically symmetric, and thus, there are no differences between $\widetilde{\rho}$ in the northern and southern hemisphere, the odd harmonics ($n = 3, 5, 7 \ldots$) resulting from the solid-body vanish due to P_n being an asymmetric function around the equator.

[6] Estimating the dynamical part of the density requires knowledge of the zonal velocity structure. Since the planet is rapidly rotating, Coriolis accelerations are dominant over the inertial accelerations (small Rossby number), and therefore, surfaces of constant angular momentum per unit mass will be nearly parallel to the axis of rotation [*Kaspi et al.*, 2009; *Schneider and Liu*, 2009]. This results in no interior flow crossing surfaces of constant angular momentum, thus to leading order the fluid motion can be only along cylinders parallel to the axis of rotation. If the fluid have been completely barotropic, this would result in a Taylor–Proudman state [*Taylor*, 1923; *Pedlosky*, 1987], where the cloud-level zonal winds extend at a constant velocity into the interior along the direction of the spin axis [*Busse*, 1976]. However, since the convectively driven interior can have baroclinic latitudinal entropy gradients resulting in thermal wind shear [*Kaspi*, 2008; *Kaspi et al.*, 2009], and due to Ohmic dissipation caused by the magnetic field [*Liu et al.*, 2008], a decay in wind velocity is expected at some depth. Thus, the zonal wind profile can take the general form

$$u(r,\theta) = u_0 e^{-\left(\frac{a-r}{H}\right)}, \tag{2}$$

where $u_0(r,\theta)$ are the observed cloud-level zonal winds extended constantly along the direction of the axis of rotation, and H is an e-folding decay depth of the cloud-level winds. The depth H is a free parameter, intended to parameterize the wind shear along the direction of angular momentum contours, and varying it systematically allows therefore investigating the dependence of the gravity harmonics on the vertical extent of the winds. Thus, the larger H is, the deeper the winds extend into the interior. Previous studies inferring dynamically induced gravity harmonics [e.g., *Hubbard*, 1999; *Kaspi et al.*, 2010; *Liu et al.*, 2013], have used only

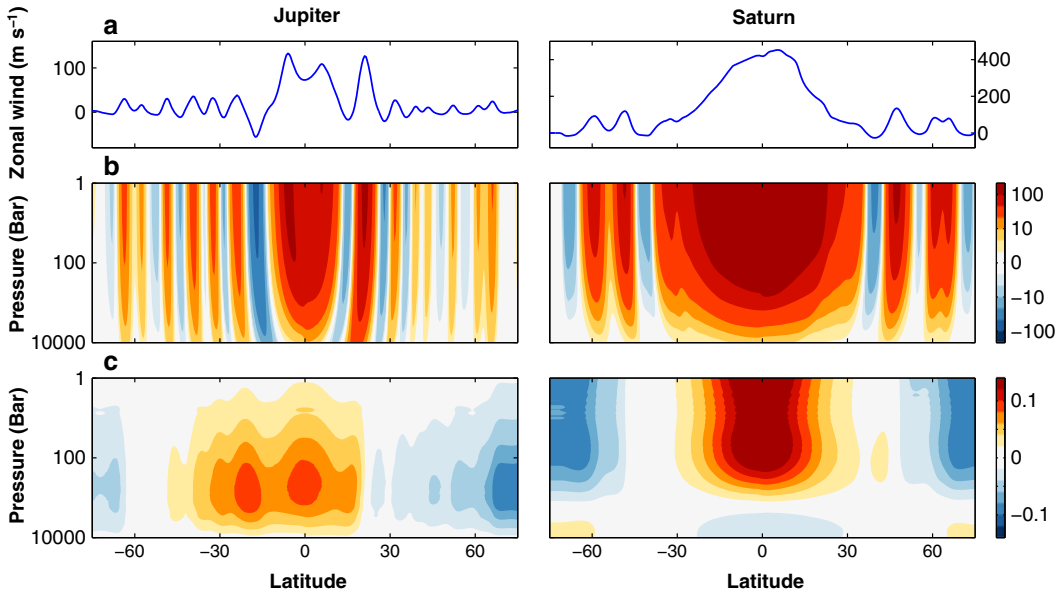

Figure 2. (a) The cloud-level zonal wind (m s^{-1}) on Jupiter [*Porco et al.*, 2003] and Saturn [*Sanchez-Lavega et al.*, 2000]. (b) The cloud-level zonal wind (m s^{-1}) as function of latitude and pressure extended along the direction of the spin axis with a decay depth of $H = 1000$ km. The color scale is logarithmic to allow resolving the high latitude jets. (c) The corresponding dynamical density anomaly, ρ', (kg m^{-3}), derived from equation 3, and set to have a zero mean.

hemispherically symmetric forms of such winds around the equator; however, since here we are interested in the asymmetric components of the gravity harmonics resulting from north–south wind asymmetries this assumption is relaxed. To avoid discontinuities across the equatorial plane, we limit the values of H to values where $H \ll a$, and use smoothed functions around the equator. It is possible to construct more sophisticated velocity profiles (e.g., H values that vary with latitude); however, the purpose of this analysis is to point that measurable odd gravity harmonics can exist due to atmospheric dynamics, and therefore, exploring a broader range of models is left for a forthcoming study. Figure 2b shows such a wind structure for a case with $H = 1000$ km for both Jupiter and Saturn (note that color scale is logarithmic). The winds at 1 bar match the observed winds (Figure 2a) and are extended into the interior (equation 2). In this Cartesian projection, deep winds become tilted equatorward because of the alignment in the direction of the spin axis.

[7] Since the dynamics are in the regime of small Rossby numbers, the flow to leading order is in geostrophic balance, and therefore, the thermal wind balance must hold so that

$$(2\boldsymbol{\Omega}\cdot\nabla)[\widetilde{\rho}\mathbf{u}] = \nabla\rho' \times \mathbf{g}_0, \tag{3}$$

where $\boldsymbol{\Omega}$ is the planetary rotation rate, $\mathbf{u}(\mathbf{r})$ is the full 3D velocity, and $\mathbf{g}_0(\mathbf{r})$ is the mean gravity vector [*Pedlosky*, 1987; *Kaspi et al.*, 2009]. Here the thermal wind balance is written in a general form without making any assumptions on the depth of the circulation [*Kaspi et al.*, 2009]. Thus, given the mean state density $\widetilde{\rho}$ from interior models [e.g., *Guillot and Morel*, 1995; *Helled et al.*, 2009], the mean gravity $\mathbf{g}_0$ (which is calculated by integrating $\widetilde{\rho}$), and the zonal velocity from equation 2, the dynamical density gradient can be calculated, and will depend only on the decay parameter H. We can to a good approximation use spherical geometry for the dynamical part of the density because the dynamics are a perturbation to the mean hydrostatic state, and thus, for the dynamics, the planet's deviation from spherical geometry is a second order effect. Thus, for the purpose of this calculation, we treat the static part of the density as only a function of radius $\widetilde{\rho} = \widetilde{\rho}(r)$. Since in spherical geometry $\widetilde{\rho}(r)$ has no projection on the Legendre Polynomials in equation 1, the static gravity harmonics, which are dominated by the oblate shape of the planet, must be calculated by other methods [e.g., *Zharkov and Trubitsyn*, 1978; *Kong et al.*, 2012; *Hubbard*, 2012].

[8] For the dynamical part of the density, equation 3 can be integrated in spherical coordinates at every vertical level to determine the dynamical density up to an integration constant. Thus, integrating equation 3 for the whole planet allows determining $\rho'(r,\theta)$ up to a nonunique function of the radius, $\rho'_0(r)$. However, this function, which physically represents a perturbation to the horizontal-mean radial density profile due to dynamics, will not contribute to the gravity harmonics since it is only a function of radius and therefore has no projection on the Legendre polynomials in equation 1. Therefore, for the purpose of determining the dynamical gravity harmonics, the choice of $\rho'_0(r)$ does not affect our results. One needs to consider though whether ρ'_0 would have had a contribution to the harmonics in the oblate system (in a similar manner to $\widetilde{\rho}$). However, for small Rossby numbers, ρ'_0 is small compared to the solid body radial density profile ($\rho'_0 \ll \widetilde{\rho}$, [*Pedlosky*, 1987]) and cannot be larger than ρ', and therefore, given the uncertainty in the profile of $\widetilde{\rho}$ itself [*Guillot*, 2005; *Helled et al.*, 2009; *Nettelmann et al.*, 2012], ρ'_0 will be within the uncertainty range of $\widetilde{\rho}$. Figure 2c shows the resulting density perturbation balancing the velocity profile in Figure 2b, with $\rho'_0(r)$ chosen such that the density perturbation has a zero mean. Then, using spherical coordinates, the dynamically induced gravity harmonics due to the density anomaly ρ' are

$$\Delta J_n = -\frac{1}{Ma^n}\int_0^a r'^{n+2}dr'\int_0^{2\pi}d\phi'\int_{-1}^{1}P_n(\mu')\rho'(r',\mu')d\mu', \tag{4}$$

where ϕ is longitude and $\mu = \cos\theta$. Figure 3 shows the gravity spectrum resulting from both the static density field (squares), and the dynamically induced gravity (circles) for cases of five different decay scale heights for both Jupiter and Saturn.

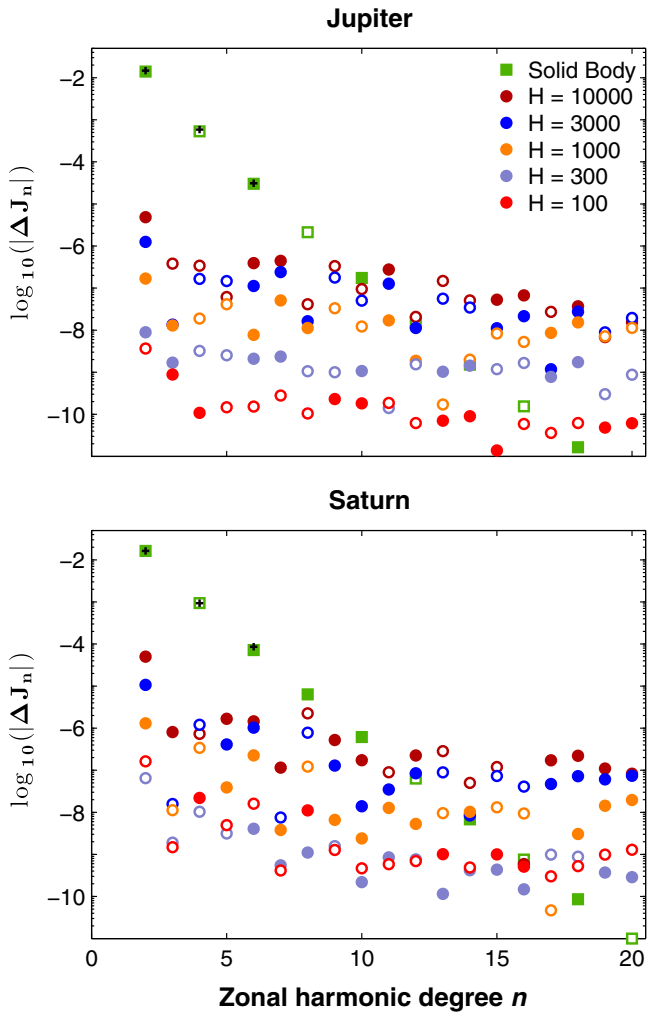

Figure 3. The static (squares) and dynamical (circles) gravity spectrum for Jupiter (top) and Saturn (bottom). The dynamical gravity harmonics (ΔJ_n) are shown for five different decay depth values: $H = 100$ km (red), $H = 300$ km (purple), $H = 1000$ km (orange), $H = 3000$ km (blue), and $H = 10000$ km (maroon). Filled (open) symbols indicate positive (negative) zonal harmonics. Black plus signs show the observed values of J_n. The static values [*Hubbard*, 1999, and W. Hubbard, personal communication] have only even components (odd harmonics are identically zero).

[9] From an inertial reference frame, the dynamics on Jupiter and Saturn are only small perturbation to the total solid-body rotation of the planets. Therefore, the low order harmonics due to solid-body rotation are orders of magnitude larger than the dynamically induced gravity harmonics (compare green squares to colored circles for $n \leq 8$ in Figure 3). Beyond $n = 10$, the gravity response due to dynamics is larger than the solid-body response. Generally, the deeper the dynamics extend, the stronger the dynamically induced gravity harmonics are, because more mass is involved in the flow. Therefore, larger H values have a generally stronger gravity response (Figure 3), though this relation is not monotonic because of the complex shape of the wind structure when projected in cylindrical symmetry (equation 2). Typically, the dynamical harmonics on Saturn are larger than they are on Jupiter because the winds are stronger and the planet is smaller (equation 4). Nonetheless, since Saturn is also more oblate than Jupiter, the static harmonics are also larger, and therefore, the ratio of dynamic to static harmonics remains roughly similar to that of Jupiter. The calculations presented here use the Voyager rotation period for Saturn (10.657 hours). The Cassini measurements have suggested an uncertainty of about 10 minutes in the exact rotation of Saturn [*Gurnett et al.*, 2007]. Therefore, all the calculations here have been repeated for this range of rotation periods (varying $\mathbf{\Omega}$ and correspondingly $\widetilde{\rho}$ [*Helled et al.*, 2009] and the zonal velocity in reference to the new rotating frame), but the results for the odd harmonics do not vary considerably.

[10] In the rotating reference frame, there are strong north–south symmetries in the wind patterns (Figure 2a), and therefore, the first even harmonics are larger than the odd harmonics ($\Delta J_2 > \Delta J_3$). For larger n due to the more complex shape of the Legendre polynomials, these differences diminish. On Jupiter, the largest asymmetry is due to the strong eastward jet at 23°N and the strong westward jet at 19°S (Figures 1 and 2a). On Saturn, the general pattern is more hemispherically symmetric (Figure 2a), but since the overall wind is stronger and the planet is smaller, Saturn has a larger J_3 and J_5 when the winds are deep. Figure 4 shows the first three odd harmonics J_3, J_5, and J_7 as function of the decay depth H.

3. Implications for the Juno and Cassini Solstice Missions

[11] One of the prime goals of the Juno mission is to determine the depth to which the cloud-level atmospheric circulation extends on Jupiter. The Cassini proximal orbits should be able to detect similar information for Saturn. It has been assumed that this will require determining the high-order even gravity harmonics at least up to J_{12} [*Hubbard*, 1999; *Kaspi et al.*, 2010; *Liu et al.*, 2013]. However, this work shows that this might be better done by measuring the odd gravity harmonics J_3, J_5 and J_7 due to several advantages over measuring the even harmonics: first, based on the dynamical thermal wind model presented here, the signal from the low-order odd harmonics is typically larger than the high-order even harmonics signal (Figure 3). Second, since the solid-body contribution to the odd harmonics is zero, there will be no need to separate out the dynamical signal from the solid-body signal, or assume some known model for the solid-body part of the harmonics. Any odd harmonic signal will be purely dynamical. Third, lower harmonics have less latitudinal variations and therefore easier to detect both spatially and temporally. This is particularly important due to the fact that any close flying probe can have only partial latitudinal coverage close to periapse where the gravity signal is largest. This work therefore proposes that detecting the gravity harmonics arising from the north–south asymmetry in the wind structure can be a superior way for detecting the depth of the zonal jets over detecting the symmetric high-order gravity signal.

[12] The sensitivity for resolving gravity harmonics diminishes with the order of the harmonics. Estimates for the sensitivity of Juno [*Finocchiaro and Iess*, 2010] show that J_3 and J_5 will be determined at a level better than 10^{-9}, while the sensitivity to even harmonics of $n > 10$ will be at the level of 2×10^{-8} or larger. Based on the results presented in Figure 4 for Jupiter, $|J_3| > 10^{-9}$ for $H > 165$ km (~ 40 bars), and $|J_5| > 10^{-9}$ for $H > 210$ km (~75 bars) (ignoring the jumps due to changes of sign). Therefore, by measuring J_3, winds extending to depths of 40 bars or more should be detectable by Juno. Note that strong winds (160 m s^{-1}) at

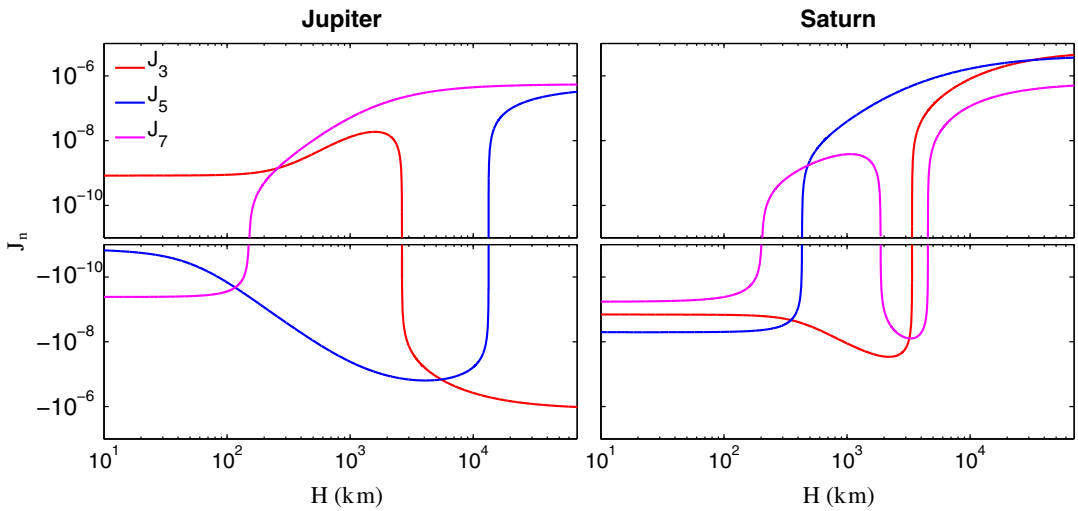

Figure 4. The odd zonal harmonics J_3, J_5, and J_7 as function of the decay scale height H for Jupiter (left) and Saturn (right). The bottom half of the plot is the negative of the log scale to reflect the negative values on a log scale. For lower values of H (not shown), all J_n values converge to zero.

nearly this pressure (22 bar) were already measured directly by the Galileo probe [*Atkinson et al*., 1996]. Alternatively, focusing on the even harmonics, as has been suggested previously, would be sensitive only to winds which are deeper than 1000 km (~5000 bars). For the case of Cassini, the ratio of the low-order odd harmonics to high-order even harmonics on Saturn is similar to that of Jupiter, and therefore, focusing on the odd harmonics for Saturn should be advantageous as well. An alternative approach to gravity harmonics analysis for detecting deep dynamics can be through direct detection of the gravity on the spacecraft (see Figure 4 in *Kaspi et al*., 2010). Then, in a similar way to the analysis presented here, hemispherical differences in the wind profile produce gravity anomalies which are greater than 1 mgal, and thus should be detectable by a close flying probe.

[13] **Acknowledgments.** I thank Adam Showman and the Juno gravity team for helpful discussions during the preparation of this work, Keke Zhang and an anonymous reviewer for very insightful reviews, and the support of the Juno project and the Helen Kimmel Center for Planetary Science at the Weizmann Institute of Science.

References

Atkinson, D. H., J. B. Pollack, and A. Seiff (1996), Galileo doppler measurements of the deep zonal winds at Jupiter, *Science*, *272*, 842–843.

Bolton, S. J. (2005), Juno final concept study report, *Tech. Rep. AO-03-OSS-03*, New Frontiers, NASA.

Busse, F. H. (1976), A simple model of convection in the Jovian atmosphere, *Icarus*, *29*, 255–260.

Finocchiaro, S., and L. Iess (2010), Numerical simulations of the gravity science experiment of the Juno mission to Jupiter, in Spaceflight mechanics 2010, vol. 136, pp. 1417–1426, American Astronomical Society.

Guillot, T. (2005), The interiors of giant planets: Models and outstanding questions, *Ann. Rev. Earth Planetary Sci.*, *33*, 493–530.

Guillot, T., and P. Morel (1995), CEPAM: a code for modeling the interiors of giant planets, *Astron. Astrophys. Suppl. Ser.*, *109*, 109–123.

Gurnett, D. A., A. M. Persoon, W. S. Kurth, J. B. Groene, T. F. Averkamp, M. K. Dougherty, and D. J. Southwood (2007), The variable rotation period of the inner region of Saturn's plasma disk, *Science*, *316*, 442–445.

Helled, R., G. Schubert, and J. D. Anderson (2009), Empirical models of pressure and density in Saturn's interior: Implications for the helium concentration, its depth dependence, and Saturn's precession rate, *Icarus*, *199*, 368–377.

Hubbard, W. B. (1984), Planetary interiors, New York, Van Nostrand Reinhold Co., 1984, 343 p.

Hubbard, W. B. (1999), Note: Gravitational signature of Jupiter's deep zonal flows, *Icarus*, *137*, 357–359.

Hubbard, W. B. (2012), High-precision Maclaurin-based models of rotating liquid planets, *Astrophys. J. Let.*, *756*, L15.

Jacobson, R. A. (2003), JUP230 orbit solutions, http://ssd.jpl.nasa.gov/.

Jacobson, R. A., et al. (2006), The gravity field of the Saturnian system from satellite observations and spacecraft tracking data, *Astrophys. J.*, *132*, 2520–2526.

Kaspi, Y. (2008), Turbulent convection in rotating anelastic spheres: A model for the circulation on the giant planets, Ph.D. thesis, Massachusetts Institute of Technology.

Kaspi, Y., G. R. Flierl, and A. P. Showman (2009), The deep wind structure of the giant planets: Results from an anelastic general circulation model, *Icarus*, *202*, 525–542.

Kaspi, Y., W. B. Hubbard, A. P. Showman, and G. R. Flierl (2010), Gravitational signature of Jupiter's internal dynamics, *Geophys. Res. Lett.*, *37*, L01204.

Kong, D., K. Zhang, and G. Schubert (2012), On the variation of zonal gravity coefficients of a giant planet caused by its deep zonal flows, *Astrophys. J.*, *748*:143.

Liu, J., P. M. Goldreich, and D. J. Stevenson (2008), Constraints on deep-seated zonal winds inside Jupiter and Saturn, *Icarus*, *196*, 653–664.

Liu, J., T. Schneider, and Y. Kaspi (2013), Predictions of thermal and gravitational signals of Jupiter's deep zonal winds, *Icarus*, in press.

Nettelmann, N., A. Becker, B. Holst, and R. Redmer (2012), Jupiter models with improved Ab initio hydrogen equation of state (H-REOS.2), *Astrophys. J.*, *750*, 52.

Pedlosky, J. (1987), *Geophysical Fluid Dynamics*, Springer, New York.

Porco, C. C., et al. (2003), Cassini imaging of Jupiter's atmosphere, satellites and rings, *Science*, *299*, 1541–1547.

Sanchez-Lavega, A., J. F. Rojas, and P. V. Sada (2000), Saturn's zonal winds at cloud level, *Icarus*, *147*, 405–420.

Schneider, T., and J. Liu (2009), Formation of jets and equatorial superrotation on Jupiter, *J. Atmos. Sci.*, *66*, 579–601.

Seidelmann, P. K., et al. (2007), Report of the IAU/IAG Working Group on cartographic coordinates and rotational elements: 2006, *CeMDA*, *98*, 155–180.

Taylor, G. I. (1923), Experiments on the motion of solid bodies in rotating fluids, *Roy. Soc. Lond. Math. Phys. Sci.*, *104*, 213–218.

Vasavada, A. R., and A. P. Showman (2005), Jovian atmospheric dynamics: An update after Galileo and Cassini, *Reports of Prog. Phys.*, *68*, 1935–1996.

Zharkov, V. N., and V. P. Trubitsyn (1978), *Physics of Planetary Interiors*, pp. 388. Pachart Publishing House, Tucson, AZ.